

A well-conditioned direct PinT algorithm for first- and second-order evolutionary equations

Jun Liu · Xiang-Sheng Wang · Shu-Lin Wu ·
Tao Zhou

the date of receipt and acceptance should be inserted later

Abstract In this paper, we propose a direct parallel-in-time (PinT) algorithm for time-dependent problems with first- or second-order derivative. We use a second-order boundary value method as the time integrator that leads to a tridiagonal time discretization matrix. Instead of solving the corresponding all-at-once system iteratively, we diagonalize the time discretization matrix, which yields a direct parallel implementation across all time levels. A crucial issue on this methodology is how the condition number of the eigenvector matrix V grows as n is increased, where n is the number of time levels. A large condition number leads to large roundoff error in the diagonalization procedure, which could seriously pollute the numerical accuracy. Based on a novel connection between the characteristic equation and the Chebyshev polynomials, we present explicit formulas for computing V and V^{-1} , by which we prove that $\text{Cond}_2(V) = \mathcal{O}(n^2)$. This implies that the diagonalization process is well-conditioned and the roundoff error only increases moderately as n grows and thus, compared to other direct PinT algorithms, a much larger n can be used to yield satisfactory parallelism. Numerical results on parallel machine are given to support our findings, where over 60 times speedup is achieved with 256 cores.

Keywords Direct PinT algorithm · Diagonalization technique · Condition number · Wave-type equations

J. Liu
Department of Mathematics and Statistics, Southern Illinois University Edwardsville, Edwardsville, IL 62026, USA.
E-mail: juliu@siue.edu

X. Wang
Department of Mathematics, University of Louisiana at Lafayette, Lafayette, LA 70503, USA.
E-mail: xswang@louisiana.edu

S. L. Wu (Corresponding author)
School of Mathematics and Statistics, Northeast Normal University, Changchun 130024, China.
E-mail: wushulin84@hotmail.com

T. Zhou
LSEC, Institute of Computational Mathematics and Scientific/Engineering Computing, AMSS, Chinese Academy of Sciences, Beijing, 100190, China.
E-mail: tzhou@lsec.cc.ac.cn

1 Introduction

For time evolutionary problems, parallelization along the time direction is an active research topic in recent years. This is driven by the fact that in modern supercomputer the number of cores (or threads) grows rapidly year by year, but in many cases one observes that the space parallelization does not bring further speedup even with more cores. When such a saturation occurs, it is natural to ask whether the time direction can be used for further speedup or not. The answer is positive, at least for strongly dissipative problems, for which the widely used parareal algorithm [28] and many other variants (e.g., the MGRiT algorithm [14] and the PFASST algorithm [13]) work very well. However, for wave propagation problems the performance of these mainstream algorithms is somewhat disappointing, because the convergence rate heavily depends on the dissipativity (see [38, 39] for discussions). There are also many efforts toward ameliorating the convergence behavior of the iterative PinT algorithms via improving the coarse grid correction [8, 10, 15, 33, 37], but as pointed out in [36] these modified algorithms either need significant additional computation burden (leading to further degradation of efficiency) or have very limited applicability.

Non-iterative (or direct) PinT algorithms are also proposed in recent years, for which the parallelism depends on the number of time points only. Here, we are interested in the PinT algorithm based on the *diagonalization* technique, which was first proposed by Maday and Rønquist [30]. The idea can be described conveniently for linear ODE system with initial-value condition (the nonlinear case will be addressed in Section 2):

$$u'(t) + Au(t) = g, \quad (1.1)$$

where $u(0) = u_0 \in \mathbb{R}^m$ is the initial condition, $A \in \mathbb{R}^{m \times m}$ and g is a known term. First, we discretize the temporal derivative by some numerical scheme (e.g., the backward-Euler method as described below), but instead of solving the difference equations sequentially one by one we formulate them into an all-at-once system

$$\mathcal{M}u := (B \otimes I_x + I_t \otimes A)u = b, \quad (1.2)$$

where $I_x \in \mathbb{R}^{m \times m}$, $I_t \in \mathbb{R}^{n \times n}$ are identity matrices and $B \in \mathbb{R}^{n \times n}$ is the time discretization matrix. (Here and hereafter n denotes the number of time points.) Then, assuming B is diagonalizable, i.e., $B = VDV^{-1}$ with $D = \text{diag}(\lambda_1, \lambda_2, \dots, \lambda_n)$, we can factorize \mathcal{M} as

$$\mathcal{M} = (V \otimes I_x)(D \otimes I_x + I_t \otimes A)(V^{-1} \otimes I_x).$$

This leads to the following three-step procedure for solving (1.2):

$$\begin{cases} \mathbf{g} = (V^{-1} \otimes I_x)\mathbf{b}, & \text{step-(a),} \\ (\lambda_j I_x + A)w_j = g_j, \quad j = 1, 2, \dots, n, & \text{step-(b),} \\ \mathbf{u} = (V \otimes I_x)\mathbf{w}, & \text{step-(c),} \end{cases} \quad (1.3)$$

where $\mathbf{w} = (w_1^\top, w_2^\top, \dots, w_n^\top)^\top$ and $\mathbf{g} = (g_1^\top, g_2^\top, \dots, g_n^\top)^\top$. For the first and third steps in (1.3), we only need to do matrix-vector (or matrix-matrix) multiplications that are parallelizable. For a fine spatial mesh, the major computational cost is to solve the n linear systems in step-(b), but these systems are completely decoupled and therefore can be solved directly in parallel.

The remaining question is how to efficiently and accurately diagonalize the time discretization matrix B . We mention that the matrix B from standard discretization may be not diagonalizable. For example, for the backward-Euler method using a uniform step-size Δt the

matrix B reads

$$B = \frac{1}{\Delta t} \begin{bmatrix} 1 & & & \\ -1 & 1 & & \\ & \ddots & \ddots & \\ & & -1 & 1 \end{bmatrix}, \quad (1.4a)$$

and it is clear that B can not be diagonalized. (For other time-integrators, e.g., the multistep methods, B is a lower triangular Toeplitz matrix and can not be diagonalized as well.) To let B diagonalizable, a natural strategy is to use variable step-sizes $\{\Delta t_j\}_{j=1}^n$, for which

$$B = \begin{bmatrix} \frac{1}{\Delta t_1} & & & \\ -\frac{1}{\Delta t_2} & \frac{1}{\Delta t_2} & & \\ & \ddots & \ddots & \\ & & -\frac{1}{\Delta t_n} & \frac{1}{\Delta t_n} \end{bmatrix}. \quad (1.4b)$$

In general, we can only rely on numerical diagonalization of B in (1.4b), but this will lead to very large condition number of the eigenvector matrix V . A large condition number results in large roundoff error in the implementation of step-(a) and step-(c) of (1.3) due to floating point operations, which could seriously pollute the accuracy of the obtained numerical solution. This issue was carefully justified by Gander *et al.* in [19] and in particular

$$\text{roundoff error} = \mathcal{O}(\epsilon \text{Cond}_2(V)), \quad (1.5)$$

where ϵ is the machine precision. In [19], the authors considered the geometrically increasing step-sizes $\{\Delta t_j = \Delta t_1 \tau^{n-j}\}_{j=1}^n$ and with this choice an explicit diagonalization of B can be written down, where $\tau > 1$ is a parameter. However, it is very difficult to make a good choice of τ : if τ tends to 1 the matrix B tends to non-normal and thus the condition number of the eigenvector matrix V becomes very large; if τ is far larger than 1 the global discretization error will be an issue, because the step-sizes grows rapidly as n increases. To balance the roundoff error and the discretization error, numerical results indicate that n can be only about 20~25 (see the numerical results in Section 4.1) and therefore the parallelism is limited.

Here, we relax the restriction on n by using a hybrid time discretization consisting of a centered finite difference scheme for the first $(n-1)$ time steps and an implicit Euler method for the last step, that is

$$\begin{cases} \frac{u_{j+1} - u_{j-1}}{2\Delta t} + Au_j = g_j, & j = 1, 2, \dots, n-1, \\ \frac{u_n - u_{n-1}}{\Delta t} + Au_n = g_n. \end{cases} \quad (1.6)$$

Such a time discretization can not be used in a time-stepping fashion, due to the serious stability problem. For (1.6), the all-at-once form of (1.2) is specified by

$$B = \frac{1}{\Delta t} \begin{bmatrix} 0 & \frac{1}{2} & & \\ -\frac{1}{2} & 0 & \frac{1}{2} & \\ & \ddots & \ddots & \ddots \\ & & -\frac{1}{2} & 0 & \frac{1}{2} \\ & & & -1 & 1 \end{bmatrix}, \quad \mathbf{b} = \begin{bmatrix} \frac{u_0}{2\Delta t} + g_1 \\ g_2 \\ \vdots \\ g_n \end{bmatrix}, \quad \mathbf{u} = \begin{bmatrix} u_1 \\ u_2 \\ \vdots \\ u_n \end{bmatrix}, \quad (1.7)$$

where only the initial-value u_0 is needed and all time steps are solved in one-shot. We mention that there are other diagonalization-based PinT algorithms, which use novel preconditioning tricks to handle the all-at-once system (1.2) and perform well for large n ; see, e.g., [6, 11, 20, 27, 29, 31]. These are however iterative algorithms and are not within the scope of this paper.

The time discretization (1.6) is not new and according to our best knowledge it is first proposed in 1985 by Axelsson and Verwer [1], where the authors studied this scheme with the aim of circumventing the well-known Dahlquist-barriers between convergence and stability which arise in using (1.6) in a time-stepping mode. In the general nonlinear case, they proved that the numerical solutions obtained simultaneously are of uniform second-order accuracy (see Theorem 4 in [1]), even though the last step is a first-order method. Numerical results in [1] indicate that the time discretization (1.6) is suitable for stiff problems in both linear and nonlinear cases. Besides (1.6), a very similar time discretization investigated by Fox in 1954 [16] and Fox and Mitchell in 1957 [17] appears much earlier, where instead of the backward-Euler method the authors use the BDF2 method for the last step in (1.6):

$$\frac{3u_n - 4u_{n-1} + u_{n-2}}{2\Delta t} + Au_n = g_n.$$

However, in this case the resulting time discretization matrix B loses the tridiagonal structure and some desirable properties which are useful to efficiently handle the all-at-once system do not hold any more. This issue was carefully justified by Brugnano, Mazzia and Trigiante in 1993 [2], who focus on solving the all-at-once system (1.2) iteratively by constructing some effective preconditioner. The implementation of the preconditioner in [2] relies on two operations: a block odd-even cyclic reduction of \mathcal{M} and a scaling procedure for the resulted matrix by its diagonal blocks. The block cyclic reduction requires matrix-matrix multiplications concerning A and the scaling requires to invert $I_x + 4\Delta t^2 A$ and $I_x + 2\Delta t A(I_x + \Delta t A)$. Both operations are expensive if A arises from semi-discretizing a PDE in high dimension and/or with fine mesh sizes. Nowadays, the hybrid time discretization (1.6) is a famous example of the so-called *boundary value methods* (BVMs) [3].

Inspired by the pioneering work by Maday and Rønquist [30], in this paper we try to solve the all-at-once system (1.2) directly (instead of iteratively as in [2]) based on diagonalizing the time discretization matrix B in (1.7) as $B = VDV^{-1}$. By a novel connection between the characteristic equation and the Chebyshev polynomials, we present explicit formulas for these three matrices V , V^{-1} and D . With the given formulas of V and V^{-1} , we prove that the condition number of V satisfies $\text{Cond}_2(V) = \mathcal{O}(n^2)$ and this implies that the roundoff error arising from the diagonalization procedure only increases moderately as n grows. Hence, compared to the algorithm in [19] a much larger n can be used to yield satisfactory parallelism in practice. We mention that the spectral decomposition algorithm developed in this paper is much faster than the benchmarking algorithm as implemented in MATLAB's `eig` function.

For second-order problems

$$u''(t) + Au(t) = g, \quad u(0) = u_0, u'(0) = \tilde{u}_0, \quad (1.8a)$$

we prove in Section 2.2 that time discretization (1.6) leads to the following all-at-once system

$$(B_{2\text{nd}} \otimes I_x + I_t \otimes A)\mathbf{u} = \mathbf{b}, \quad (1.8b)$$

where \mathbf{b} is a suitable vector (see Lemma 2.1 for details) and the matrix $B_{2\text{nd}}$ satisfies

$$B_{2\text{nd}} = B^2, \quad (1.9)$$

with B being the time discretization matrix of (1.6) for the first-order problems (cf. (1.7)). Thus, the same diagonalization of B with squared eigenvalues, i.e., $B_{2\text{nd}} = VD^2V^{-1}$, can be directly reused and the condition number of the eigenvector matrix is not effected.

The left of this paper is organized as follows. In Section 2 we introduce the direct PinT algorithm for nonlinear problems. In Section 3 we show details of the diagonalization of the time discretization matrix B in (1.7), which plays a central role for both the linear and nonlinear cases. Our numerical results are given in Section 4 and we conclude this paper in Section 5. The technical details for estimating $\text{Cond}_2(V)$ are given in Appendix A and a fast algorithm with complexity $\mathcal{O}(n^2)$ for stably computing V^{-1} is given in Appendix B.

2 The PinT algorithm for nonlinear problems

In this section, we introduce the time discretization and the diagonalization-based PinT algorithm for nonlinear problems. We will consider differential equations with first- and second-order temporal derivatives separately.

2.1 First-order problems

We first consider the following first-order problem

$$u'(t) + f(u(t)) = 0, u(0) = u_0, \quad (2.1)$$

where $t \in (0, T)$, $u(t) \in \mathbb{R}^m$ and $f : (0, T) \times \mathbb{R}^m \rightarrow \mathbb{R}^m$. This is an ODE problem, but the algorithm described below is directly applicable to semi-discretized time-dependent PDEs. For example, (2.1) corresponds to the heat equations by letting $f(u) = Au$ with $A \in \mathbb{R}^{m \times m}$ being the discrete matrix of the negative Laplacian $-\Delta$ by any discretization (e.g. finite difference or finite element). Similarly, the second-order problems considered in subsection 2.2 corresponds to the wave equations.

For (2.1), similar to (1.6) the time discretization scheme is

$$\begin{cases} \frac{u_{j+1} - u_j}{2\Delta t} + f(u_j) = 0, & j = 1, 2, \dots, n-1, \\ \frac{u_n - u_{n-1}}{\Delta t} + f(u_n) = 0, \end{cases} \quad (2.2)$$

where the last step is the first-order backward-Euler scheme. The all-at-once system of (2.2) is

$$(B \otimes I_x) \mathbf{u} + F(\mathbf{u}) = \mathbf{b}, \quad (2.3)$$

where $F(\mathbf{u}) = (f^\top(u_1), f^\top(u_2), \dots, f^\top(u_n))^\top$ and $\mathbf{b} = (u_0^\top/(2\Delta t), 0, \dots, 0)^\top$. To solve (2.3), we use the simplified Newton's iteration described in [18]. To this end, we first consider standard Newton's iteration applied to (2.3):

$$(B \otimes I_x + \nabla F(\mathbf{u}^k))(\mathbf{u}^{k+1} - \mathbf{u}^k) = \mathbf{b} - ((B \otimes I_x) \mathbf{u}^k + F(\mathbf{u}^k)),$$

i.e.,

$$(B \otimes I_x + \nabla F(\mathbf{u}^k)) \mathbf{u}^{k+1} = \mathbf{b} + (\nabla F(\mathbf{u}^k) \mathbf{u}^k - F(\mathbf{u}^k)), \quad (2.4)$$

where $k \geq 0$ is the iteration index and $\nabla F(\mathbf{u}^k) = \text{blkdiag}(\nabla f(u_1^k), \dots, \nabla f(u_n^k))$ consists of the Jacobian matrix $\nabla f(u_j^k)$ as the j -th block. Define the averaged Jacobian matrix¹

$$A^k = \frac{1}{n} \sum_{j=1}^n \nabla f(u_j^k).$$

Then, by replacing each $\nabla f(u_j^k)$ by A^k we get an approximation of $\nabla F(\mathbf{u}^k)$ as

$$\nabla F(\mathbf{u}^k) \approx I_t \otimes A^k.$$

By substituting this into (2.4) we arrive at the simplified Newton iteration (SNI):

$$(B \otimes I_x + I_t \otimes A^k) \mathbf{u}^{k+1} = \mathbf{b} + ((I_t \otimes A^k) \mathbf{u}^k - F(\mathbf{u}^k)). \quad (2.5)$$

Convergence of SNI is well-known; see, e.g., [12, Theorem 2.5] and [34]. The SNI was also used as an inner iteration for the inexact Uzawa method [32] and the Krylov subspace method [29].

¹ An alternative way of deriving such an aggregated Jacobian matrix is to take the average of unknowns instead: $A^k = \nabla f\left(\frac{1}{n} \sum_{j=1}^n u_j^k\right)$, which is omitted since it shows similar convergence performance in numerical experiments.

If B is diagonalizable as $B = VDV^{-1}$, we can solve \mathbf{u}^{k+1} in (2.5) as

$$\begin{cases} \mathbf{g} = (V^{-1} \otimes I_x) \mathbf{r}^k, & \text{step-(a),} \\ (\lambda_j I_x + A_k) w_j = g_j, \quad j = 1, 2, \dots, n, & \text{step-(b),} \\ \mathbf{u}^{k+1} = (V \otimes I_x) \mathbf{w}, & \text{step-(c),} \end{cases} \quad (2.6)$$

where $\mathbf{r}^k = \mathbf{b} + ((I_t \otimes A_k - F(\mathbf{u}^k)))$. In the linear case, i.e., $f(u) = Au$, we have $A_k = A$ and $\mathbf{r}^k = \mathbf{b}$ and therefore (2.6) reduces to (1.3). For each SNI, the Jacobian system (2.5) can be solved in parallel.

2.2 Second-order problems

We next consider the following second-order differential equation

$$u''(t) + f(u(t)) = 0, u(0) = u_0, u'(0) = \tilde{u}_0, t \in (0, T). \quad (2.7)$$

For discretization we first make an *order-reduction* by rewriting (2.7) as

$$\begin{bmatrix} u(t) \\ v(t) \end{bmatrix}' = \begin{bmatrix} v(t) \\ -f(u(t)) \end{bmatrix}, \quad u(0) = u_0, v(0) = \tilde{u}_0. \quad (2.8)$$

Let $w(t) = (u^\top(t), v^\top(t))^\top$ and $g(w) = (v^\top(t), -f^\top(u(t)))^\top$. Then, similar to (2.2) we have

$$\begin{cases} \frac{w_{j+1} - w_{j-1}}{2\Delta t} + g(w_j) = 0, \quad j = 1, 2, \dots, n-1, \\ \frac{w_n - w_{n-1}}{\Delta t} + g(w_n) = 0. \end{cases} \quad (2.9)$$

Then, the all-at-once system is of the same form as in (2.3) and the diagonalization procedure (2.6) is directly applicable. But one can imagine that the storage requirement for the space variables doubles at each time point and this would be a problem if the second-order problem (2.7) arises from semi-discretizing a PDE in high dimension and/or with fine mesh sizes. We avoid this by representing the all-at-once systems for $\mathbf{u} = (u_1, u_2, \dots, u_n)^\top$ only.

Lemma 2.1 (all-at-once system for \mathbf{u}) *The vector $\mathbf{u} = (u_1^\top, \dots, u_n^\top)^\top$ specified by the time discretization (2.9) satisfies*

$$(B^2 \otimes I_x) \mathbf{u} + F(\mathbf{u}) = \mathbf{b}, \quad (2.10)$$

where B is the matrix defined by (1.7) and $\mathbf{b} = \left(\frac{\tilde{u}_0^\top}{2\Delta t}, -\frac{u_0^\top}{4\Delta t^2}, 0, \dots, 0 \right)^\top$.

If $f(u) = Au$, we have $F(\mathbf{u}) = (f^\top(u_1), \dots, f^\top(u_n))^\top = (I_t \otimes A) \mathbf{u}$ and thus the all-at-once system (2.10) for \mathbf{u} becomes $(B^2 \otimes I_x + I_t \otimes A) \mathbf{u} = \mathbf{b}$, which gives (1.8b).

Proof. Since $w_j = (u_j^\top, v_j^\top)^\top$, from (2.9) we can represent $\{u_j\}$ and $\{v_j\}$ separately as

$$\begin{cases} \frac{u_{j+1} - u_{j-1}}{2\Delta t} - v_j = 0, \quad j = 1, 2, \dots, n-1, \\ \frac{u_n - u_{n-1}}{\Delta t} - v_n = 0, \\ \frac{v_{j+1} - v_{j-1}}{2\Delta t} + f(u_j) = 0, \quad j = 1, 2, \dots, n-1, \\ \frac{v_n - v_{n-1}}{\Delta t} + f(u_n) = 0. \end{cases}$$

Hence, with the matrix B given by (1.7) we have

$$(B \otimes I_x) \mathbf{u} - \mathbf{v} = \mathbf{b}_1, \quad (B \otimes I_x) \mathbf{v} + F(\mathbf{u}) = \mathbf{b}_2, \quad (2.11)$$

where $\mathbf{v} = (v_1^\top, \dots, v_n^\top)^\top$, $\mathbf{b}_1 = \left(\frac{u_0^\top}{2\Delta t}, 0, \dots, 0 \right)^\top$ and $\mathbf{b}_2 = \left(\frac{\tilde{u}_0^\top}{2\Delta t}, 0, \dots, 0 \right)^\top$. From the first equation in (2.11) we have $\mathbf{v} = (B \otimes I_x) \mathbf{u} - \mathbf{b}_1$ and substituting this into the second equation gives $(B \otimes I_x)^2 \mathbf{u} + F(\mathbf{u}) = \mathbf{b}_2 + (B \otimes I_x) \mathbf{b}_1$. A routine calculation yields $\mathbf{b}_2 + (B \otimes I_x) \mathbf{b}_1 = \mathbf{b}$ and this together with $(B \otimes I_x)^2 = B^2 \otimes I_x$ gives the desired result (2.10). ■

Clearly, $B_{2\text{nd}} := B^2$ is diagonalizable as $B_{2\text{nd}} = VD^2V^{-1}$ given $B = VDV^{-1}$. Based on this relationship, it is clear that the above PinT algorithm (2.6) is also applicable to (2.11) and the details are therefore omitted. Hence the computational cost of second-order problems is the same as the first-order ones.

3 Diagonalization of the time discretization matrix B

For both the linear and nonlinear problems, it is clear that the diagonalization of $B = VDV^{-1}$ plays a central role in the PinT algorithm. In this section, we will prove that the matrix B is indeed diagonalizable and also give explicit formulas for V and V^{-1} . By these formulas, we given an estimate of 2-norm condition number of V , i.e., $\text{Cond}_2(V) = \mathcal{O}(n^2)$, which is critical to control the roundoff error in practical computation (cf. (1.5)).

For simplicity, we consider the diagonalization of the re-scaled matrix $\mathbb{B} = \Delta t B$. Clearly, by diagonalizing $\mathbb{B} = V\Sigma V^{-1}$ it holds

$$B = \frac{1}{\Delta t} \mathbb{B} = V \left(\frac{1}{\Delta t} \Sigma \right) V^{-1} = VDV^{-1}.$$

Define two functions

$$T_n(x) = \cos(n \arccos x), \quad U_n(x) = \sin[(n+1) \arccos x] / \sin(\arccos x),$$

which are respectively the n -th degree Chebyshev polynomials of the first- and second-kind. In the following theorem we express the eigenvalues and eigenvectors of \mathbb{B} through the Chebyshev polynomials. Throughout this paper, $i = \sqrt{-1}$ denotes the imaginary unit.

Theorem 3.1 *The eigenvalues of \mathbb{B} are $\lambda_j = ix_j$, with $\{x_j\}_{j=1}^n$ being the n roots of*

$$U_{n-1}(x) - iT_n(x) = 0. \quad (3.1)$$

For each λ_j , the corresponding eigenvector $\mathbf{p}_j = [p_{j,0}, \dots, p_{j,n-1}]^T$ is given as

$$p_{j,k} = i^k U_k(x_j), \quad k = 0, \dots, n-1, \quad (3.2)$$

where $p_{j,0} = 1$ is assumed for normalization.

Proof. Let $\lambda \in \mathbb{C}$ be an eigenvalue of \mathbb{B} and $\mathbf{p} = [p_0, p_1, \dots, p_{n-1}]^T \neq 0$ is the corresponding eigenvector. By definition we have $\mathbb{B}\mathbf{p} = \lambda\mathbf{p}$, i.e.,

$$\begin{cases} \lambda p_0 = p_1/2, \\ \lambda p_1 = -p_0/2 + p_2/2, \\ \vdots \\ \lambda p_{n-2} = -p_{n-3}/2 + p_{n-1}/2, \\ \lambda p_{n-1} = -p_{n-2} + p_{n-1}. \end{cases} \quad (3.3)$$

Obviously, $p_0 \neq 0$; otherwise, $p_1 = \dots = p_{n-1} = 0$. Without loss of generality, we may assume $p_0 = 1$. Clearly, p_k is a polynomial of λ with degree k . Moreover, $p_1 = 2\lambda$ and the recursion

$$2\lambda p_{k-1} = p_k - p_{k-2}, \quad (3.4)$$

holds for $k = 2, \dots, n-1$, and the last equation gives

$$(1 - \lambda)p_{n-1} = p_{n-2}. \quad (3.5)$$

Let $\lambda = \frac{1}{2}(y - \frac{1}{y}) = i \cos \theta$ with $y = ie^{i\theta}$. A general solution of the difference equation (3.4) is

$$p_k = c_1 y^k + c_2 / (-y)^k. \quad (3.6)$$

Making use of the initial conditions $p_0 = 1$ and $p_1 = 2\lambda = y - 1/y$, we have

$$c_1 + c_2 = 1, \quad c_1 y - c_2 / y = y - 1/y,$$

which gives $c_1 = \frac{y}{y+1/y}$ and $c_2 = \frac{1/y}{y+1/y}$. Therefore, with $y = ie^{i\theta}$ we get

$$p_k = \frac{y^{k+1} + (-1)^k / y^{k+1}}{y + 1/y} = \frac{i^k \sin[(k+1)\theta]}{\sin \theta}, \quad k = 0, \dots, n-1. \quad (3.7)$$

In view of $\lambda = i \cos \theta$, we rewrite (3.5) as

$$(1 - i \cos \theta) \frac{i^{n-1} \sin(n\theta)}{\sin \theta} = \frac{i^{n-2} \sin[(n-1)\theta]}{\sin \theta},$$

which is equivalent to

$$\frac{\sin(n\theta)}{\sin \theta} = i \cos(n\theta). \quad (3.8)$$

This is a polynomial equation of $\lambda = i \cos \theta$ with degree n .

Denote $\lambda = ix$ with $x = \cos \theta$ (i.e. $\theta = \arccos x$). It follows from (3.7) and (3.8) that

$$p_k = i^k U_k(x), \quad k = 0, 1, \dots, n-1, \quad (3.9)$$

and

$$U_{n-1}(x) - iT_n(x) = 0. \quad (3.10)$$

The n roots x_1, x_2, \dots, x_n of (3.10) give the n eigenvalues $\lambda_j = ix_j$ of \mathbb{B} , and the formula (3.9) evaluated at each x_j then provides the corresponding eigenvector. ■

Based on the above Theorem 3.1, we can further prove that \mathbb{B} is indeed diagonalizable, since its eigenvalues are all distinct.

Theorem 3.2 *All n roots of $U_{n-1}(x) - iT_n(x) = 0$ are simple, complex with negative imaginary parts, and have modulus less than $1 + 1/\sqrt{2n}$. Moreover, if x is a root, then so is $-\bar{x}$.*

Proof. From (3.1), it is clear that $U_{n-1}(x) - iT_n(x) = 0$ has no real roots. Define $y = x + \sqrt{x^2 - 1}$ for $x \in \mathbb{C} \setminus [-1, 1]$. It holds $x = (y + 1/y)/2$ and $|y| > 1$. Moreover,

$$T_n(x) = (y^n + 1/y^n)/2, \quad U_{n-1}(x) = (y^n - 1/y^n)/(y - 1/y).$$

Thus, if $U_{n-1}(x) - iT_n(x) = 0$, we have $(y^n - 1/y^n)/(y^n + 1/y^n) = (y - 1/y)/(-2i)$, which gives

$$y^{2n} = \frac{-2i + y - 1/y}{-2i - y + 1/y} = -\frac{y^2 - 2iy - 1}{y^2 + 2iy - 1} = -\frac{(y - i)^2}{(y + i)^2}. \quad (3.11)$$

Since $|y| > 1$, we have $|y - i| > |y + i|$; namely, the imaginary part $\text{Im } y < 0$. Consequently,

$$\text{Im } x = \frac{\text{Im } y - \text{Im } y/|y|}{2} < 0. \quad (3.12)$$

Moreover, it follows from (3.11) that

$$|y|^{2n} = \frac{|y - i|^2}{|y + i|^2} \leq \frac{(|y| + 1)^2}{(|y| - 1)^2}.$$

Let $y_1 = |y| - 1 > 0$. We then have

$$2 + y_1 \geq y_1(1 + y_1)^n \geq y_1(1 + ny_1) = y_1 + ny_1^2,$$

which implies $y_1 \leq \sqrt{2/n}$. Thus, $|x| < \frac{|y|+1}{2} \leq 1 + \frac{1}{\sqrt{2n}}$. If x is a root, then

$$U_{n-1}(-\bar{x}) = (-1)^{n-1} \bar{U}_{n-1}(x) = (-1)^{n-1} (-i) \bar{T}_n(x) = iT_n(-\bar{x}),$$

which implies that $-\bar{x}$ is also a root. A simple application of Pythagorean theorem yields

$$T_n^2(x) + (1 - x^2)U_{n-1}^2(x) = 1. \quad (3.13)$$

Hence, if x is a root of $U_{n-1}(x) - iT_n(x) = 0$, it holds $x^2 T_n^2(x) = 1$. If x were a repeated root, then

$$2xT_n^2(x) + 2x^2T_n(x)T_n'(x) = 0.$$

Since $T_n'(x) = nU_{n-1}(x)$, we have

$$T_n(x) = -nxU_{n-1}(x) = -inxT_n(x),$$

which implies $x = i/n$ and this contradicts to the fact that $\text{Im } x < 0$. \blacksquare

By Theorem 3.2, the eigenvectors of \mathbb{B} are linearly independent and so \mathbb{B} indeed is diagonalizable. Denote the spectral decomposition of \mathbb{B} by $\mathbb{B} = V\Sigma V^{-1}$ with $\Sigma = \text{diag}(\lambda_1, \lambda_2, \dots, \lambda_n)$ and

$$V = [\mathbf{p}_1, \mathbf{p}_2, \dots, \mathbf{p}_n] = \underbrace{\text{diag}(i^0, i^1, \dots, i^{n-1})}_{:=\mathbf{I}} \underbrace{\begin{bmatrix} U_0(x_1) & \cdots & U_0(x_n) \\ \vdots & \cdots & \vdots \\ U_{n-1}(x_1) & \cdots & U_{n-1}(x_n) \end{bmatrix}}_{:=\Phi} = \mathbf{I}\Phi, \quad (3.14)$$

where $\{\lambda_j\}_{j=1}^n$ and $\{x_j\}_{j=0}^{n-1}$ are the quantities specified by Theorem 3.1. In (3.14), \mathbf{I} is a unitary matrix and Φ is a Vandermonde-like matrix [26] defined by the Chebyshev orthogonal polynomials. Hence, it holds

$$\text{Cond}_2(V) = \text{Cond}_2(\mathbf{I}\Phi) = \text{Cond}_2(\Phi). \quad (3.15)$$

The following theorem indicates that $\text{Cond}_2(V) = \mathcal{O}(n^2)$, which implies that the roundoff error from diagonalization procedure only increases moderately as n grows (cf. (1.5)). Such a property of $\text{Cond}_2(V)$ is crucial to achieve a high massively parallel efficiency in time.

Theorem 3.3 For $n \geq 8$, it holds

$$\text{Cond}_2(V) = \mathcal{O}(n^2). \quad (3.16)$$

Proof. From (3.15), the proof lies in proving $\text{Cond}_2(\Phi) = \mathcal{O}(n^2)$ by using the Christoffel-Darboux formula and some special properties of relevant orthogonal polynomials. The details are rather technical and are given in Appendix A. \blacksquare

An interesting byproduct of Appendix A is the precise estimate of each individual eigenvalue of \mathbb{B} , which allows us to accurately compute all eigenvalues by Newton's method with $\mathcal{O}(n)$ complexity.

Remark 3.1 (fast algorithm for V^{-1}) Making use of the special structure of Φ (cf. (3.14)), in Appendix B we designed a new stable and fast algorithm with complexity $\mathcal{O}(n^2)$ for computing V^{-1} . We believe that this algorithm is of independent interest since it provides a very different methodology for inverting the Vandermonde-like matrix, which is a well-known ill-conditioned problem and there are a lot of researches in this filed, such as [7, 21–23, 25, 35] to name a few. We present some numerical results in Section 4.2 to demonstrate the efficiency of the proposed algorithm.

4 Numerical results

In this section, we present numerical examples to illustrate the advantage of our proposed direct PinT solver, with respect to numerical accuracy, stable spectral decomposition and parallel efficiency. For the first two parts, the results are obtained by using MATLAB on a laptop PC with Intel(R) Core(TM) i7-7700HQ CPU@2.80GHz CPU and 32GB RAM. For parallel computation, we use a parallel computer (SIUE Campus Cluster) with 10 CPU nodes connected via 25-Gigabit per second (Gbps) Ethernet network, where each node is equipped with two AMD EPYC 7F52 16-Core Processors at 3.5GHz base clock and 256GB RAM. For the complex-shift linear systems in step-(b) of our direct PinT solver (cf. (1.3)), we use the LU factorization-based direct solver provided as PCLU preconditioner in PETSc. In parallel examples, let $J(n, s)$ be the measured CPU (wall-clock) time by using s cores for n time points. Following the standard measures [5, 9] of parallel scalability, we compute the parallel speedup as the ratio

$$\text{Speedup (Sp.)} = \frac{J(n, 1)}{J(n, s)}.$$

The strong and weak scaling efficiency with s cores are computed as

$$\text{Strong Efficiency (SE)} = \frac{J(n, 1)}{s \times J(n, s)}, \quad \text{Weak Efficiency (WE)} = \frac{J(2, 1)}{J(2 \times s, s)}.$$

We highlight that the measured parallel speedup and efficiency are affected by many factors, such as computer cluster setting and how to implement the parallel codes. Hence our parallel results may largely underestimate the best possible speedup and efficiency with optimized parallel codes.

4.1 Accuracy comparison of two direct PinT algorithms

As mentioned in Section 1, the direct PinT algorithm based on the diagonalization technique was first proposed in [19], where the authors used the geometrically increasing step-sizes $\Delta t_j = \Delta t_n \tau^{j-n}$ to make the time discretization matrix B diagonalizable. Compared to their algorithm, the most important advantage of our PinT algorithm lies in the much weaker dependence of the roundoff error (due to diagonalization) on n . The first set of numerical results are devoted to comparing such a dependence for these two algorithms. To this end, we consider the following 1D wave equation

$$u_{tt} - u_{xx} = 0, \quad u(x, 0) = \sin(2\pi x), \quad u'(x, 0) = 0, \quad (x, t) \in (-1, 1) \times (0, T), \quad (4.1)$$

with periodic boundary condition $u(-1, t) = u(1, t)$. Applying the centered finite difference method in space with a uniform mesh $\{x_j = j\Delta x\}_{j=1}^m$ gives the following second-order ODE system

$$\mathbf{u}_h'' + A\mathbf{u}_h = 0, \quad \mathbf{u}_h(0) = \mathbf{u}_{0,h}, \quad \mathbf{u}_h'(0) = 0, \quad t \in (0, T), \quad (4.2)$$

where

$$A = \frac{1}{\Delta x^2} \begin{bmatrix} 2 & -1 & & -1 \\ -1 & 2 & -1 & \\ & \ddots & \ddots & \ddots \\ & & -1 & 2 & -1 \\ -1 & & & -1 & 2 \end{bmatrix}, \quad \mathbf{u}_{0,h} = \begin{bmatrix} \sin(2\pi x_1) \\ \sin(2\pi x_2) \\ \vdots \\ \sin(2\pi x_m) \end{bmatrix}, \quad \Delta x = \frac{2}{m}.$$

For (4.2), the diagonalization-based PinT algorithm in [19] uses the Trapezoidal rule (TR) as the time-integrator, where the step-sizes are fixed by $\Delta t_j = \Delta t_n \tau^{j-n}$ for $j = 1, 2, \dots, n$ with $\tau > 1$ being a constant and Δt_n being given a prior. Let $\Delta x = \frac{1}{64}$, $\Delta t_n = 10^{-2}$ and $\tau = 1.15$. We let n vary from 4 to 50 and for each n we implement the diagonalization-based algorithm in [19] by using the variable step-sizes. Then, we calculate the length of the time interval, i.e., $T(\tau, n) = \sum_{j=1}^n \Delta t_j$ ¹ and implement the algorithm proposed in this paper by using a uniform step-size $\Delta t = T(\tau, n)/n$. Define the global error of numerical solution as

$$\text{global error} = \max_{j=1,2,\dots,n} \|\mathbf{u}_{j,h} - \mathbf{u}_{j,h}^{\text{ref}}\|_{\infty}, \quad (4.3)$$

where $\{\mathbf{u}_{j,h}^{\text{ref}}\}$ denotes the reference solution obtained by using the `expm` function in MATLAB. The sequence $\{\mathbf{u}_{j,h}\}$ is obtained via three ways: by the algorithm studied in this paper, by the algorithm in [19] and by the time-stepping TR using the variable step-sizes.

In Figure 4.1 on the left, we compare the global error for these three numerical solutions and it is clear that for the algorithm in [19] the quantity n can not be large and the error grows rapidly when $n > 25$. As denoted by the black solid line, the error of the time-stepping TR does not change dramatically as n increases and this is because for each n the last step-size Δt_n (i.e., the largest step-size) is fixed. For the time-stepping TR, the global error is just the time discretization error. By comparing the dash-dot blue line (with marker ‘o’) with the black solid line, we can see how the roundoff error affects the global error: when n is small the roundoff error is smaller than the time discretization error and therefore the influence of the roundoff error is invisible, but when n is large (say $n > 25$) the roundoff error plays a dominate role and blows up as n increases. From [19], we know that such a rapid increase of the roundoff error is due to the very large condition number of \tilde{V} . Indeed, as we can see in Figure 4.1 on the right, such a condition number becomes very large as n grows. On the contrary, the condition number for the new algorithm only moderately increases as n grows and it is much smaller. Such a moderate condition number can be used to explain As shown in Figure 4.1 on the left, the global error of the new algorithm never blows up and in fact it continuously decrease when $n \geq 6$. Such a phenomenon confirms the condition number very well, because a moderate condition number implies that the roundoff error is much smaller than the time discretization error and thus the global error is dominated by the time discretization error. The decreasing of the global error can be explained as follows. The step-size

$$\Delta t = \Delta t_n \sum_{j=1}^n \tau^{j-n} / n = \Delta t_n \frac{1 - \tau^{-n}}{n(1 - \tau^{-1})} \approx \frac{0.0766}{n} \quad (\text{if } n \geq 40)$$

decreases as n grows and thus the time discretization error decreases accordingly.

4.2 Fast algorithms for spectral decomposition of \mathbb{B} .

The spectral decomposition of the time discretization matrix $B = VDV^{-1}$ is important in our PinT algorithm. The eigenvalue λ_j can be computed by Newton’s method described as follows. Based on Theorem 3.1 it holds $\lambda_j = i \cos(\theta_j)$, where θ_j is the j -th root of $\rho(\theta) := \sin(n\theta) - i \cos(n\theta) \sin \theta = 0$ (cf. (3.8)). Applying Newton’s iteration to $\rho(\theta)$ leads to

$$\theta_j^{(l+1)} = \theta_j^{(l)} - \frac{\rho(\theta_j^{(l)})}{\rho'(\theta_j^{(l)})}, \quad l = 0, 1, 2, \dots \quad (4.4)$$

¹ For the algorithm in [19], since $\Delta t_j = \Delta t_n \tau^{j-n}$ the length of time interval grows as n increases.

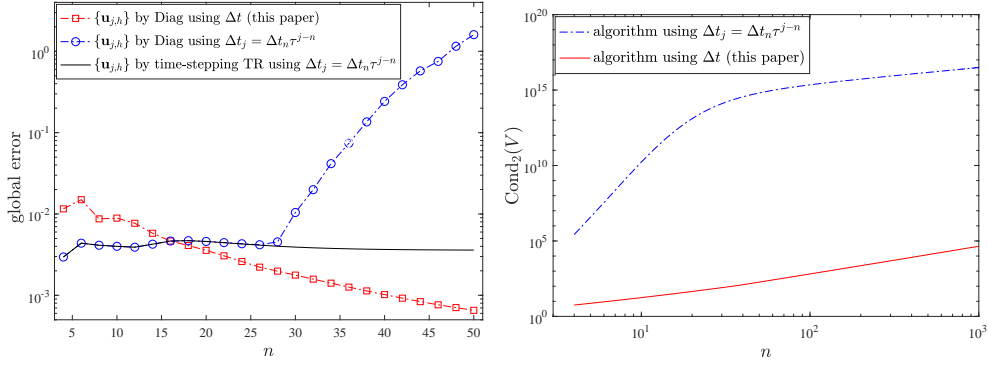


Fig. 4.1 Left: the global error for the new algorithm studied in this paper, the algorithm in [19] and the time-stepping TR using the variable step-sizes. Right: comparison of the condition numbers of the eigenvector matrix V for the two diagonalization-based algorithms.

Such a Newton method runs n loops for the n eigenvalues λ_j 's. The maximal iteration number over all the n eigenvalues is almost constant and therefore the complexity of Newton's iteration (4.4) for computing all the eigenvalues is of $\mathcal{O}(n)$, which is significantly faster than the standard QR algorithm with $\mathcal{O}(n^3)$ complexity as used by MATLAB's highly optimized built-in function `eig`. However, it is rather difficult to choose the n initial guesses $\{\theta_j^{(0)}\}_{j=1}^n$. If these initial guesses are not properly chosen, the n iterates $\{\theta_j^{(l)}\}_{j=1}^n$ converge to \tilde{n} different values with $\tilde{n} < n$, i.e., not all the eigenvalues are founded (because the n eigenvalues are different). By Lemma A.1, we suggest using

$$\theta_j^{(0)} = \frac{1}{2} \left(\frac{j\pi}{n} + \frac{j\pi}{n+1} \right) + \frac{i}{n}, \quad j = 1, 2, \dots, n.$$

by which the iterates of (4.4) converge to the n different eigenvalues correctly.

For V^{-1} , we also proposed a fast algorithm with complexity $\mathcal{O}(n^2)$ in Appendix B, which is of independent interest in the area of numerical methods for Vandermonde-like matrices. The advantage of explicitly constructing the inverse matrix V^{-1} is to increase the parallel efficiency of step-(a) by reducing communication cost. Let $B = V_{\text{eig}} D_{\text{eig}} V_{\text{eig}}^{-1}$ and $B = V_{\text{fast}} D_{\text{fast}} V_{\text{fast}}^{-1}$ be the computed spectral decomposition of B by the `eig` function and our fast algorithm (implemented with MATLAB), respectively. Define the maximum relative difference between the eigenvalues (sorted in the same order)

$$\eta_{\text{fast}} := \|D_{\text{eig}} - D_{\text{fast}}\|_F / \|D_{\text{eig}}\|_F,$$

and the norm of relative residuals (measures the overall accuracy of the spectral decompositions)

$$\omega_{\text{eig}} := \|B - V_{\text{eig}} D_{\text{eig}} V_{\text{eig}}^{-1}\|_F / \|B\|_F, \quad \omega_{\text{fast}} := \|B - V_{\text{fast}} D_{\text{fast}} V_{\text{fast}}^{-1}\|_F / \|B\|_F.$$

Here, we show CPU time (in seconds) estimated by the timing functions `tic/toc` in MATLAB for such a spectral decomposition. For comparison, we also show the CPU time for the `eig` function in MATLAB. In Table 4.1, we compare the computational time and the approximation accuracy for the `eig` function (for computing V_{eig} and Σ_{eig}) and `inv` function (for computing V_{eig}^{-1}) in MATLAB and our proposed fast spectral decomposition algorithm, where the column 'Iter' denotes the number of Newton iterations required to reach the tolerance `tol` = 10^{-10} . The CPU time of our fast algorithm shows $\mathcal{O}(n^2)$ growth, which is significantly less than that

of the `eig` function (with $O(n^3)$ growth). In particular, for $n = 8192$ we observed more than 25 times speedup. Moreover, the eigenvalues and eigenvectors computed by these two methods are essentially the same, if we take into account the effects of roundoff errors.

Table 4.1 Comparison of `eig+inv` function and our fast spectral decomposition algorithm

n	MATLAB's <code>eig+inv</code>		Our fast algorithm			
	CPU	ω_{eig}	Iter	CPU	ω_{fast}	η_{fast}
64	0.009	1.64e-14	7	0.009	3.61e-13	2.67e-15
128	0.049	6.56e-14	7	0.022	1.06e-12	4.58e-15
256	0.149	1.54e-13	8	0.020	1.10e-11	6.09e-15
512	0.348	8.27e-13	8	0.072	5.30e-11	2.69e-14
1024	1.304	3.37e-12	9	0.273	2.04e-10	1.02e-13
2048	7.542	1.23e-11	9	1.152	5.12e-10	2.54e-13
4096	55.877	1.28e-09	10	4.551	6.75e-09	5.60e-13
8192	459.947	1.73e-08	10	17.898	2.85e-08	1.34e-12

4.3 Parallel Experiments

In this subsection, we provide a series of parallel results to validate the speedup and parallel efficiency of our direct PinT algorithm.

Example-1. In this example we consider a 2D heat equation with homogeneous Dirichlet boundary condition defined on a square domain $\Omega = (0, \pi)^2$:

$$\begin{cases} u_t(x, y, t) - \Delta u(x, y, t) = r(x, y, t), & \text{in } \Omega \times (0, T), \\ u(x, y, t) = 0, & \text{on } \partial\Omega \times (0, T), \\ u(x, y, 0) = u_0(x, y), & \text{in } \Omega, \end{cases} \quad (4.5)$$

where $u_0(x, y) = \sin(x)\sin(y)$ and $r(x, y, t) = \sin(x)\sin(y)e^{-t}$. The exact solution of this problem is $u(x, y, t) = \sin(x)\sin(y)e^{-t}$. Approximating Δ by a centered finite difference scheme with a uniform mesh step size $h = \pi/(N+1)$ in both x and y directions gives the following ODE system:

$$\mathbf{u}'_h(t) - \Delta_h \mathbf{u}_h(t) = \mathbf{r}_h(t), \quad \mathbf{u}_h(0) = \mathbf{u}_{0,h},$$

where $\Delta_h \in \mathbb{R}^{N^2 \times N^2}$ is the 5-point stencil Laplacian matrix, \mathbf{u}_h , \mathbf{r}_h , $\mathbf{u}_{0,h}$ denotes the finite difference approximation to the corresponding u , r , u_0 over the $m = N \times N$ interior spatial grid points. In Table 4.2, we show the approximation errors (measured by the ∞ -norm) and the strong and weak scaling results of our direct PinT solver, where the spatial mesh size is fixed to be $N = 512$ and the number of cores ranges from 1 to 256. The approximation errors in weak scaling results show a second-order accuracy in time before dominated by the discretization errors in space. Both strong and weak scaling efficiency are very promising up to 32 cores. But when the core number ≥ 64 , we see an obvious drop of the parallel efficiency. This is mainly due to our slow interconnect between the nodes (each node contains 32 cores). Using a fast, low-latency interconnect (e.g., the InfiniBand networking based on remote direct memory access (RDMA) technology) would greatly further improve the parallel efficiency. Notice the discretized all-at-once linear system with a $N^2 \times n = 512^3$ space-time mesh has more than 134 million unknowns and by using 256 cores it can be solved in about 20 seconds, rather than over 20 mins using a single core.

Table 4.2 Scaling results of example 1: a heat PDE ($T = 2$ with $N = 512$)

Core#	strong scaling					weak scaling			
s	n	Error	CPU	Sp.	SE	n	Error	CPU	WE
1	512	2.23e-06	1318.8	1.0	100.0%	2	7.93e-02	5.4	100.0%
2	512	2.23e-06	667.8	2.0	98.7%	4	1.19e-02	5.4	100.0%
4	512	2.23e-06	346.4	3.8	95.2%	8	3.22e-03	5.4	100.0%
8	512	2.23e-06	173.0	7.6	95.3%	16	8.26e-04	5.5	98.2%
16	512	2.23e-06	90.7	14.5	90.9%	32	2.09e-04	5.8	93.1%
32	512	2.23e-06	51.1	25.8	80.7%	64	5.28e-05	6.6	81.8%
64	512	2.23e-06	32.0	41.2	64.4%	128	1.37e-05	8.3	65.1%
128	512	2.23e-06	23.0	57.3	44.8%	256	4.25e-06	12.0	45.0%
256	512	2.23e-06	19.4	68.0	26.6%	512	2.23e-06	19.6	27.6%

Example-2. We next consider a linear wave equation with homogeneous Dirichlet boundary condition defined on a 2D square domain $\Omega = (0, 1)^2$:

$$\begin{cases} u_{tt}(x, y, t) - \Delta u(x, y, t) = r(x, y, t), & \text{in } \Omega \times (0, T), \\ u(x, y, t) = 0, & \text{on } \partial\Omega \times (0, T), \\ u(x, y, 0) = u_0(x, y), & \text{in } \Omega, \\ u_t(x, y, 0) = \bar{u}_0(x, y), & \text{in } \Omega, \end{cases} \quad (4.6)$$

with the following data

$$\begin{aligned} u_0(x, y) &= 0, \quad \bar{u}_0(x, y) = 2\pi x(x-1)y(y-1), \\ r(x, y, t) &= -4\pi^2 x(x-1)y(y-1) \sin(2\pi t) - 2 \sin(2\pi t)(x(x-1) + y(y-1)). \end{aligned}$$

The exact solution of this problem is $u(x, y, t) = x(x-1)y(y-1) \sin(2\pi t)$. Using the same notations in **Example-1**, we obtain a second-order ODE system:

$$\mathbf{u}_h''(t) - \Delta_h \mathbf{u}_h(t) = \mathbf{r}_h(t), \quad \mathbf{u}_h(0) = \mathbf{u}_{0,h}, \quad \mathbf{u}_h'(0) = \bar{\mathbf{u}}_{0,h},$$

where $\bar{\mathbf{u}}_{0,h}$ denotes the finite difference approximation to \bar{u}_0 over the spatial grid points. Then, we show in Table 4.3 the approximation errors, the strong and weak scaling results. The parallel efficiency is very similar to that in Table 4.2. Since our PinT algorithm is based on the same spectral decomposition $B = VDV^{-1}$, the computational cost of solving the above second-order problem is essentially the same as the first-order problem in **Example-1**. This is a desirable advantage over those iterative algorithms (e.g. parareal and MGRiT), whose convergence rates are usually much slower for handling hyperbolic problems.

Table 4.3 Scaling Results of Example 2: a wave PDE ($T = 2$ with $N = 512$)

Core#	Strong scaling					Weak scaling			
s	n	Error	CPU	Sp.	SE	n	Error	CPU	WE
1	512	7.88e-05	1328.6	1.0	100.0%	2	9.19e-03	5.4	100.0%
2	512	7.88e-05	676.3	2.0	98.2%	4	2.21e-02	5.4	100.0%
4	512	7.88e-05	332.6	4.0	99.9%	8	3.16e-01	5.5	100.0%
8	512	7.88e-05	172.6	7.7	96.2%	16	1.33e-01	5.7	100.0%
16	512	7.88e-05	91.2	14.6	91.0%	32	2.30e-02	6.0	94.8%
32	512	7.88e-05	51.7	25.7	80.3%	64	5.21e-03	7.1	82.1%
64	512	7.88e-05	31.2	42.6	66.5%	128	1.27e-03	9.5	67.9%
128	512	7.88e-05	23.2	57.3	44.7%	256	3.16e-04	14.8	46.6%
256	512	7.88e-05	20.3	65.4	25.6%	512	7.88e-05	27.4	28.2%

Example-3. At last, we consider a semi-linear parabolic equation with homogeneous Dirichlet boundary condition defined on a 2D square domain $\Omega = (-1, 1)^2$:

$$\begin{cases} u_t(x, y, t) - \Delta u(x, y, t) + f(u) = r(x, y, t), & \text{in } \Omega \times (0, T), \\ u(x, y, t) = 0, & \text{on } \partial\Omega \times (0, T), \\ u(x, y, 0) = u_0(x, y), & \text{in } \Omega, \end{cases} \quad (4.7)$$

where

$$\begin{aligned} f(u) &= u^3 - u, \quad u_0(x, y) = (x^2 - 1)(y^2 - 1), \\ r(x, y, t) &= -2(x^2 - 1)(y^2 - 1)e^{-t} + (x^2 - 1)^3(y^2 - 1)^3e^{-3t} - 2e^{-t}((x^2 - 1) + (y^2 - 1)). \end{aligned}$$

This problem has the exact solution $u(x, y, t) = (x^2 - 1)(y^2 - 1)e^{-t}$. By the centered finite difference method for spatial discretization as in the previous two examples, we get a nonlinear ODE system

$$\mathbf{u}'_h(t) - \Delta_h \mathbf{u}_h(t) + f(\mathbf{u}_h(t)) = \mathbf{r}_h(t), \quad \mathbf{u}_h(0) = \mathbf{u}_{0,h}. \quad (4.8)$$

This particular type of nonlinear function $f(u) = u^3 - u$ was widely used in literature, e.g. the Schlögl model in [4, 24]. We solve (4.8) by the nonlinear PinT algorithm described in Section 2.1, for which the simplified Newton iteration starts from a zero initial guess and stops whenever the relative residual norms is smaller than the given tolerance 10^{-8} .

In Table 4.4, we show the approximation errors and the strong and weak scaling results of the PinT algorithm, where the required number of SNI (listed in the column ‘SNI’) shows an anticipated mesh-independent convergence rate. Different from the linear examples, we see that the parallel efficiency for more than 32 cores is clearly lower. This is mainly because of the communication cost in distributing the averaged block-diagonal Jacobian matrices and dispatching the residual vectors during the sequential Newton iterations. The codes may be redesigned or further optimized for achieving better parallel efficiency, which is however beyond the scope of the current paper.

Table 4.4 Scaling Results of Example 3: a semi-linear PDE ($T = 2$ with $N = 256$)

Core#	Strong scaling						Weak scaling				
	n	Error	SNI	CPU	Sp.	SE	n	Error	SNI	CPU	WE
1	512	6.36e-07	9	1514.0	1.0	100.0%	2	4.40e-01	11	6.6	100.0%
2	512	6.36e-07	9	770.4	2.0	98.3%	4	7.64e-03	9	5.4	122.2%
4	512	6.36e-07	9	400.6	3.8	94.5%	8	2.33e-03	11	6.8	97.1%
8	512	6.36e-07	9	217.2	7.0	87.1%	16	6.38e-04	9	5.9	111.9%
16	512	6.36e-07	9	126.9	11.9	74.6%	32	1.63e-04	9	7.0	94.3%
32	512	6.36e-07	9	84.7	17.9	55.9%	64	4.07e-05	9	9.4	70.2%
64	512	6.36e-07	9	67.6	22.4	35.0%	128	1.02e-05	9	28.8	22.9%
128	512	6.36e-07	9	60.6	25.0	19.5%	256	2.55e-06	9	29.8	22.1%
256	512	6.36e-07	9	60.8	24.9	9.7%	512	6.36e-07	9	61.6	10.7%

5 Conclusions

In this paper we developed and analyzed a diagonalization-based non-iterative PinT algorithm for the first-order and second-order evolutionary problems. The algorithm is based on using a second-order boundary value problem as the time integrator and diagonalizing the time discretization matrix. The explicit spectral decomposition of the time discretization matrix is given and we prove that condition number of the eigenvector matrix is of order $\mathcal{O}(n^2)$. The weaker dependence of the condition number on n guarantees that the proposed algorithm can

be used to handle a larger number of time points, compared to a closely related algorithm by Gander *et al.* [19]. For implementing the algorithm, we need to compute the inverse of the eigenvector matrix, for which we give a fast algorithm with complexity $\mathcal{O}(n^2)$ by exploiting the special structures of the matrices. Numerical results indicate that the new algorithm has promising advantages with respect to roundoff errors and practical parallel speedup.

Appendix A: estimate the condition number of V .

The proof of Theorem 3.3 is based on the following lemmas. Recall the following definitions: $i = \sqrt{-1}$ is the imaginary unit and

$$T_n(x) = \cos(n \arccos x), \quad U_n(x) = \sin[(n+1) \arccos x] / \sin(\arccos x),$$

are the n -th degree Chebyshev polynomials of first and second kind, respectively. The following lemma provides some nice and frequently used properties of the zeros of the polynomial equation $U_{n-1}(x) - iT_n(x) = 0$.

Lemma A.1 *The zeros of $U_{n-1}(x) - iT_n(x) = 0$ can be arranged as x_1, \dots, x_n such that for each $j = 1, \dots, n$, $x_j = \cos(\theta_j) = \cos(\alpha_j + i\beta_j)$ with $\alpha_j = (j\pi - a_j)/n$ and $\beta_j = b_j/n$, where $a_j \in (0, \pi)$ and $b_j > 0$ satisfy the following equations*

$$|x_j| = \frac{\cosh \beta_j}{\cosh b_j} = \frac{\sin \alpha_j}{\sinh b_j} = \frac{\sinh \beta_j}{\sin a_j} = \frac{1}{\sqrt{\cos^2 a_j + \sinh^2 b_j}}, \quad \cos a_j \sinh \beta_j = \sin a_j \cos \alpha_j. \quad (\text{A.1})$$

Moreover, we have the symmetric relations

$$a_j + a_{n+1-j} = \alpha_j + \alpha_{n+1-j} = \pi, \quad b_{n+1-j} = b_j, \quad \beta_{n+1-j} = \beta_j, \quad j = 1, \dots, n, \quad (\text{A.2})$$

and the monotone properties (with $m = \lfloor n/2 \rfloor$ being the largest integer less than or equal to $n/2$)

$$0 < a_1 < \dots < a_m < \pi/2 < a_{n+1-m} < \dots < a_n < \pi, \quad 0 < b_1 < \dots < b_m, \quad (\text{A.3})$$

and the inequalities

$$b_j > \frac{1}{n}, \quad a_j < \frac{j\pi}{n+1} < \alpha_j < \frac{j\pi}{n}, \quad j = 1, \dots, m. \quad (\text{A.4})$$

If $n = 2m + 1$, then $b_{m+1} > 1/2$. If $n = 2m$, then $b_m > 1/2$.

Proof. Let $\bar{b} > 0$ be the unique positive root of the equation $\sinh b \sinh(b/n) = 1$. It is easily seen that the function

$$f(b) := n \arcsin[\tanh b \cosh(b/n)] + \arcsin[\tanh(b/n) \cosh b]$$

is strictly increasing on $[0, \bar{b}]$ with $f(0) = 0$ and $f(\bar{b}) = (n+1)\pi/2$. For each positive index $j \leq (n+1)/2$, there exists a unique $b_j \in (0, \bar{b}]$ such that $f(b_j) = j\pi$. Define

$$\beta_j = b_j/n, \quad a_j = \arcsin[\tanh(b_j/n) \cosh b_j], \quad \alpha_j = (j\pi - a_j)/n = \arcsin[\tanh b_j \cosh(b_j/n)].$$

A simple calculation shows that $x_j = \cos(\alpha_j + i\beta_j)$ is a root of $U_{n-1}(x) - iT_n(x) = 0$. Moreover, (A.1) holds for $1 \leq j \leq (n+1)/2$. For $(n+1)/2 \leq j \leq n$, define

$$b_j = b_{n+1-j}, \quad \beta_j = b_j/n = \beta_{n+1-j}, \quad a_j = \pi - a_{n+1-j}, \quad \alpha_j = (j\pi - a_j)/n = \pi - \alpha_{n+1-j}.$$

We also obtain (A.1) and $U_{n-1}(x_j) - iT_n(x_j) = 0$ with $x_j = \cos(\alpha_j + i\beta_j)$.

The symmetric properties (A.2) follows immediately from the above construction. The monotonicity of $f(b)$ on $[0, \bar{b}]$ and (A.2) imply the monotonicity of a_j and b_j in (A.3). In view of $f(1/n) > \pi$, we obtain $b_j > 1/n$. Note from (A.1) that

$$\tan a_j / \tan \alpha_j = \sinh \beta_j / \sin \alpha_j = \tanh \beta_j / \tanh b_j < 1.$$

Thus, we have $a_j < \alpha_j$. This together with $\alpha_j = (j\pi - a_j)/n$ implies $a_j < j\pi/(n+1) < \alpha_j$, and then (A.4) follows. Finally, for $n = 2m + 1$ it holds $b_{m+1} = \bar{b} > 1/2$, because $\sinh(1/2) \sinh[1/(2n)] < 1 = \sinh \bar{b} \sinh(\bar{b}/n)$. For $n = 2m$, it holds $\cos \alpha_m = \sin(a_m/n) < a_m/n < \pi/(2n)$. In view of (A.1) and $n \geq 2$, we have

$$1 = (\cos^2 \alpha_m + \sinh^2 \beta_m)(\cos^2 a_m + \sinh^2 b_m) < (0.7 + \sinh^2 b_m/4)(1 + \sinh^2 b_m),$$

which implies that $b_m > 1/2$. This completes the proof. \blacksquare

In the following, we always assume that the zeros x_j (as well as a_j, b_j, α_j and β_j) are ordered as in Lemma A.1. We denote by \bar{x}_j the conjugate of x_j . The following lemma gives some sharp bounds of the zeros, which will be used in the proof of Lemma A.3.

Lemma A.2 Assume $n \geq 3$. For any $j = 1, \dots, n$, we have

$$|x_j| > \frac{\ln n}{2n}, \quad \frac{1}{|x_j^2(\bar{x}_j - x_j)|} < n^3. \quad (\text{A.5})$$

Proof. By symmetry, we only need to consider the case $j \leq (n+1)/2$. Assume to the contrary that $|x_j| \leq (\ln n)/(2n)$ for some $j \leq (n+1)/2$. Let $\sigma = (n+1)/2 - j \geq 0$. We claim $\sigma < 1/2 + (\ln n)/4$. Otherwise, we have $j \leq n/2 - (\ln n)/4$, $\alpha_j < j\pi/n \leq \pi/2 - (\pi \ln n)/(4n)$, and consequently, $|x_j| > \cos \alpha_j > \sin[(\pi \ln n)/(4n)] > (\ln n)/(2n)$, which is a contradiction. Hence, it holds

$$\sigma < 1/2 + (\ln n)/4, \quad j > n/2 - (\ln n)/4.$$

It then follows that $\alpha_j > j\pi/(n+1) > \pi/2 - \pi(\ln n + 2)/(4n + 4)$. Thus, $\cos \alpha_j < \sin[\pi(\ln n + 2)/(4n + 4)] < \pi(\ln n + 2)/(4n + 4)$. Since $\sinh \beta_j < |x_j| \leq (\ln n)/(2n)$, we have $b_j < n \sinh \beta_j < (\ln n)/2$ and $\sinh b_j < e^{b_j}/2 < \sqrt{n}/2$. Consequently,

$$1 = (\cos^2 \alpha_j + \sinh^2 \beta_j)(\cos^2 a_j + \sinh^2 b_j) < \left(\frac{\pi^2(\ln n + 2)^2}{16(n+1)^2} + \frac{(\ln n)^2}{4n^2} \right) \left(1 + \frac{n}{4} \right),$$

which is a contradiction again. This proves the first inequality in (A.5).

Next, we note that $|\bar{x}_j - x_j| = 2|\operatorname{Im} x_j| = 2 \sin \alpha_j \sinh \beta_j$ and

$$|x_j^2(\bar{x}_j - x_j)| = 2(\cos^2 \alpha_j + \sinh^2 \beta_j) \sin \alpha_j \sinh \beta_j.$$

If $\cos^2 \alpha_j \geq 0.4$, from $\sin \alpha_j > 2\alpha_j/\pi > 2/(n+1)$ and $\sinh \beta_j > \beta_j > 1/n^2$ we have

$$\frac{1}{|x_j^2(\bar{x}_j - x_j)|} < \frac{n^2(n+1)}{1.6} < n^3.$$

If $\cos^2 \alpha_j < 0.4$, it follows from $n \geq 3$ and (A.1) that

$$1 = (\cos^2 \alpha_j + \sinh^2 \beta_j)(\cos^2 a_j + \sinh^2 b_j) < (0.4 + \sinh^2 b_j/9)(1 + \sinh^2 b_j),$$

which implies that $b_j > 0.87$ and $\sinh \beta_j > \beta_j = b_j/n > 0.87/n$. We then have

$$\frac{1}{|x_j^2(\bar{x}_j - x_j)|} < \frac{1}{2\sqrt{1-0.4}\sinh^3 \beta_j} < \frac{n^3}{2\sqrt{0.6}(0.87)^3} < n^3.$$

Coupling the above two cases yields the second inequality of (A.5). ■

The following lemma will be used to estimate $\|\Phi\|_2$.

Lemma A.3 For any $j = 1, \dots, n$, it holds

$$\frac{1}{|x_j|} \sum_{k=1}^n \left[\frac{1}{|x_k(\bar{x}_j - x_k)|} + \frac{1}{2|x_k|} \right] = \mathcal{O}(n^3). \quad (\text{A.6})$$

Proof. By symmetry, we assume $j \leq \frac{n+1}{2}$. If $k < \frac{n}{2}$, then $\operatorname{Re} x_{n+1-k} < 0 < \operatorname{Re} x_j$. Thus,

$$|\bar{x}_j - x_{n+1-k}| > |x_{n+1-k}| = |x_k| > \cos \alpha_k > \sin \frac{(n/2 - k)\pi}{n} > \frac{n - 2k}{n},$$

and

$$\sum_{k > n/2+1} \frac{1}{|x_k(\bar{x}_j - x_k)|} < \sum_{k < n/2} \frac{1}{|x_{n+1-k}(\bar{x}_j - x_{n+1-k})|} < \sum_{k < n/2} \frac{n^2}{(n - 2k)^2} < \frac{\pi^2 n^2}{6}. \quad (\text{A.7})$$

If $k < n/2$ and $k \neq j$, it holds

$$|\bar{x}_j - x_k| > 2 \sin \frac{\alpha_j + \alpha_k}{2} \sin \frac{|\alpha_j - \alpha_k|}{2} > \frac{2(j+k-1)(|j-k|-1/2)}{n^2}.$$

Therefore,

$$\sum_{k < n/2, k \neq j} \frac{1}{|x_k(\bar{x}_j - x_k)|} < \sum_{k < n/2, k \neq j} \frac{n^3}{2(n-2k)(j+k-1)(|j-k|-1/2)} = \mathcal{O}(n^2).$$

Finally, since $|x_k(\bar{x}_j - x_k)| > |\operatorname{Im} x_k|^2 = \sin^2 \alpha_k \sinh^2 \beta_k$, it is easy to estimate

$$\sum_{n/2 \leq k \leq n/2+1} \frac{1}{|x_k(\bar{x}_j - x_k)|} = \mathcal{O}(n^2). \quad (\text{A.8})$$

A combination of the above estimates and Lemma A.2 gives the desired result. \blacksquare

For each $s = 1, \dots, n$, we denote $\theta_s = s\pi/(n+1)$ and $y_s = \cos \theta_s$. Let

$$L_j(x) = \prod_{1 \leq k \leq n, k \neq j} \frac{x - x_k}{x_j - x_k} = \frac{U_{n-1}(x) - iT_n(x)}{(x - x_j)[U'_{n-1}(x_j) - iT'_n(x_j)]}, \quad (\text{A.9})$$

be the Lagrange interpolation polynomials such that $L_j(x_k) = \delta_{jk}$, where $j = 1, \dots, n$. The following lemma will be used to estimate $\|\Phi^{-1}\|_2$.

Lemma A.4 *For any $j = 1, \dots, n$, we have*

$$\sum_{s=1}^n (1 - y_s^2) |L_j(y_s)| \sum_{k=1}^n |L_k(y_s)| = \mathcal{O}(n^2). \quad (\text{A.10})$$

Proof. A routine calculation gives

$$|L_j(y_s)| = \left| \frac{(-1)^{s-1}(1 + iy_s)(1 - x_j^2)}{(y_s - x_j)(i - nx_j)x_j T_n(x_j)} \right| = \frac{|1 - x_j^2|\sqrt{1 + y_s^2}}{|(y_s - x_j)(i - nx_j)|}. \quad (\text{A.11})$$

Note that $|1 - x_j^2| = |\sin(\alpha_j + i\beta_j)|^2 = \sin^2 \alpha_j + \sinh^2 \beta_j$ and $|x_j| > \max\{|\cos \alpha_j|, \sinh \beta_j\}$. Since y_s is real with $y_s^2 < 1$ and $\operatorname{Im} x_j < 0$, we have $|y_s - x_j| \geq |\operatorname{Im} x_j| = \sin \alpha_j \sinh \beta_j$, and

$$|L_j(y_s)| < \frac{\sqrt{2}|1 - x_j^2|}{n|x_j(y_s - x_j)|} < \frac{\sqrt{2}\sin^2 \alpha_j}{n|x_j(y_s - x_j)|} + \frac{\sqrt{2}}{n \sin \alpha_j} < \frac{\sqrt{2}\sin^2 \alpha_j}{n|x_j(y_s - x_j)|} + \sqrt{2}, \quad (\text{A.12})$$

where we have used the inequality $\sin \alpha_j > \sin[\pi/(n+1)] > 2/(n+1) > 1/n$. Another application of $|y_s - x_j| > \sin \alpha_j \sinh \beta_j$ yields

$$|L_j(y_s)| - \sqrt{2} < \frac{\sqrt{2}\sin \alpha_j}{n|x_j| \sinh \beta_j} < \frac{\sqrt{2}}{n|x_j|\beta_j}.$$

If $\cos^2 \alpha_j \leq 1/2$, then (A.1) implies that $1 < (1/2 + \sinh^2 \beta_j)(1 + \sinh^2 \beta_j)$. Hence, $\beta_j > 0.4$ and $|x_j| > \sinh \beta_j > 0.4/n$. If $\cos^2 \alpha_j > 1/2$, then $|x_j| > |\cos \alpha_j| > 1/\sqrt{2}$ and $\beta_j = b_j/n > 1/n^2$. In either case, we have

$$|L_j(y_s)| - \sqrt{2} = \mathcal{O}(n), \quad 1 \leq j, s \leq n. \quad (\text{A.13})$$

We next estimate the sum $\sum_{k=1}^n |L_k(y_s)|$. By symmetry, we assume without loss of generality that $s \leq (n+1)/2$. If $k < m = \lfloor n/2 \rfloor$ and $k \neq s$, then it follows from Lemma A.1 and (A.12) that

$$|y_s - x_k| > 2 \sin \frac{\alpha_k + \theta_s}{2} \sin \frac{|\alpha_k - \theta_s|}{2} > \frac{2(\alpha_k + \theta_s)|\alpha_k - \theta_s|}{\pi^2} > \frac{2(k+s)(|k-s|-1/2)}{(n+1)^2},$$

and

$$\sum_{k=1, k \neq s}^{m-1} (\sqrt{2}|L_k(y_s)| - 2) < \sum_{k=1, k \neq s}^{m-1} \frac{(n+1)\pi^2(k+1/2)^2}{n(n+1-2k)(k+s)(|k-s|-1/2)} = \mathcal{O}(n). \quad (\text{A.14})$$

If $k > n+1-m$, then $\operatorname{Re} x_k < 0 \leq y_s$ and $|y_s - x_k| > |y_s - x_{n+1-k}|$. Moreover, $|i - nx_k| = |i - nx_{n+1-k}|$. It then follows from (A.11) that $|L_k(y_s)| < |L_{n+1-k}(y_s)|$. This together with (A.13) and (A.14) implies that

$$\sum_{k=1}^n (|L_k(y_s)| - \sqrt{2}) = \mathcal{O}(n). \quad (\text{A.15})$$

Finally, we want to estimate $\sum_{s=1}^n (1 - y_s^2) |L_j(y_s)|$. Since $|L_j(y_s)| = |L_{n+1-j}(y_{n+1-s})|$, it suffices to consider the case $j \leq (n+1)/2$; namely, $\alpha_j \leq \pi/2$. For $1 \leq s, j \leq (n+1)/2$ with $s \neq j$, we have

$$|y_s - x_j| > 2 \sin \frac{|\theta_s - \alpha_j|}{2} \sin \frac{\theta_s + \alpha_j}{2} > \frac{2(\theta_s + \alpha_j)|\theta_s - \alpha_j|}{\pi^2} > \frac{2(j+s)(|j-s|-1/2)}{(n+1)^2},$$

and $1 - y_s^2 = \sin^2 \theta_s < \theta_s^2 = s^2 \pi^2 / (n+1)^2$. It then follows from (A.12) that

$$(1 - y_s^2)(|L_j(y_s)| - \sqrt{2}) < \frac{\sqrt{2} \pi^2 s^2}{(\ln n)(j+s)(|j-s|-1/2)}.$$

By a routine calculation, we obtain from the above inequality and (A.13) that

$$\sum_{s \leq (n+1)/2} (1 - y_s^2) [|L_j(y_s)| - \sqrt{2}] = \mathcal{O}(n). \quad (\text{A.16})$$

If $s \geq (n+1)/2$, then $y_s < 0 < \operatorname{Re} x_j$ and $|y_s - x_j| > |y_s - x_{n+1-j}|$. It follows from (A.11) that $|L_j(y_s)| < |L_j(y_{n+1-s})|$. On account of $y_s = -y_{n+1-s}$, we obtain

$$\sum_{s=1}^n (1 - y_s^2) |L_j(y_s)| < 2 \sum_{s \leq (n+1)/2} (1 - y_s^2) [|L_j(y_s)| - \sqrt{2}] = \mathcal{O}(n). \quad (\text{A.17})$$

Coupling (A.15) and (A.17) gives the desired estimate. \blacksquare

Proof of Theorem 3.3.

Denote $s_k := x_k T_n(x_k)$. It is readily seen that $s_k^2 = 1$, $U_{n-1}(x_k) = i s_k / x_k$ and $U_n(x_k) = (1 + i x_k) s_k / x_k$. Recall from (3.14) that Φ is the main component of the eigenvector matrix V of \mathbb{B} . It then follows from the Christoffel-Darboux formula that

$$(\Phi^* \Phi)_{jk} = \sum_{l=0}^{n-1} U_l(\bar{x}_j) U_l(x_k) = \frac{U_n(\bar{x}_j) U_{n-1}(x_k) - U_{n-1}(\bar{x}_j) U_n(x_k)}{2(\bar{x}_j - x_k)} = \frac{s_j s_k (2i + \bar{x}_j - x_k)}{2\bar{x}_j x_k (\bar{x}_j - x_k)},$$

which together with Lemma A.3 implies

$$\sum_{k=1}^n |(\Phi^* \Phi)_{jk}| \leq \frac{1}{|x_j|} \sum_{k=1}^n \left[\frac{1}{|x_k(\bar{x}_j - x_k)|} + \frac{1}{2|x_k|} \right] = \mathcal{O}(n^3),$$

and

$$\|\Phi\|_2 = \sqrt{\rho(\Phi^* \Phi)} \leq \sqrt{\|\Phi^* \Phi\|_\infty} = \mathcal{O}(n^{3/2}). \quad (\text{A.18})$$

Let $W = (w_{jk})_{j,k=1}^n = \Phi^{-1}$. We obtain from orthogonality and Gaussian quadrature formula that

$$w_{jk} = \frac{2}{\pi} \int_{-1}^1 L_j(x) U_{k-1}(x) \sqrt{1-x^2} dx = \sum_{s=1}^n \frac{2(1-y_s^2)}{n+1} L_j(y_s) U_{k-1}(y_s), \quad (\text{A.19})$$

where $L_j(x)$ are the Lagrange interpolation polynomials given by (A.9). A simple calculation yields

$$(WW^*)_{jk} = \sum_{s=1}^n \frac{2(1-y_s^2)}{n+1} L_j(y_s) \bar{L}_k(y_s),$$

which together with Lemma A.4 implies

$$\|W\|_2 = \sqrt{\rho(WW^*)} \leq \sqrt{|WW^*|_1} = \mathcal{O}(n^{1/2}). \quad (\text{A.20})$$

Coupling (A.18) and (A.20) gives $\operatorname{Cond}_2(V) = \operatorname{Cond}_2(\Phi) = \|\Phi\|_2 \|W\|_2 = \mathcal{O}(n^2)$. \square

Appendix B: A fast $\mathcal{O}(n^2)$ algorithm for computing V^{-1} .

From (3.14), the eigenvector matrix V of \mathbb{B} satisfies $V = \mathbf{I}\Phi$ with $\mathbf{I} = \text{diag}(i^0, i^1, \dots, i^{n-1})$. In the diagonalization procedure (1.3), we need to compute $V^{-1} = \Phi^{-1}\mathbf{I}^{-1}$ and the major computation is to get $W = \Phi^{-1}$. In this appendix, we present a fast and stable $\mathcal{O}(n^2)$ algorithm for computing W accurately.

A simple application of the recurrence relation $2yU_j(y) = U_{j+1}(y) + U_{j-1}(y)$ gives

$$4y_s^2 U_{k-1}(y_s) = 2y_s[U_{k-2}(y_s) + U_k(y_s)] = \begin{cases} U_{k-3}(y_s) + 2U_{k-1}(y_s) + U_{k+1}(y_s), & 2 \leq k \leq n-1, \\ U_{k-1}(y_s) + U_{k+1}(y_s), & k = 1, \\ U_{k-3}(y_s) + U_{k-1}(y_s), & k = n. \end{cases} \quad (\text{B.1})$$

It then follows from (A.19) that

$$\begin{aligned} 2w_{jk} &= \frac{1}{n+1} \sum_{s=1}^n 4L_j(y_s)U_{k-1}(y_s) - \frac{1}{n+1} \sum_{s=1}^n 4y_s^2 L_j(y_s)U_{k-1}(y_s) \\ &= \begin{cases} 2\psi_{j,k} - \psi_{j,k-2} - \psi_{j,k+2}, & 2 \leq k \leq n-1, \\ 3\psi_{j,k} - \psi_{j,k-2}, & k = 1, \\ 3\psi_{j,k} - \psi_{j,k+2}, & k = n, \end{cases} \end{aligned} \quad (\text{B.2})$$

where $\psi_{j,k} = \frac{1}{n+1} \sum_{s=1}^n L_j(y_s)U_{k-1}(y_s)$. Since $U_n(y_s) = 0$, we have $\psi_{j,n+1} = 0$ for $j = 1, 2, \dots, n$. Define

$$p_n(x) = U_{n-1}(x) - iT_n(x), \quad b_k = \frac{1}{n+1} \sum_{s=1}^n p_n(y_s)U_{k-1}(y_s). \quad (\text{B.3})$$

Recall from (A.9) that $p_n(y_s) = p'_n(x_j)(y_s - x_j)L_j(y_s)$. Therefore,

$$\frac{2b_k}{p'_n(x_j)} = \frac{1}{n+1} \sum_{s=1}^n 2(y_s - x_j)L_j(y_s)U_{k-1}(y_s) = \psi_{j,k-1} + \psi_{j,k+1} - 2x_j\psi_{j,k}. \quad (\text{B.4})$$

To evaluate b_k , we investigate the integral of $p_n(x)U_{k-1}(x)\sqrt{1-x^2}$ on $[-1, 1]$. On account of (B.1) and (B.3), we obtain from the Gaussian quadrature formula that

$$\begin{aligned} \frac{4}{\pi} \int_{-1}^1 p_n(x)U_{k-1}(x)\sqrt{1-x^2}dx &= \frac{1}{n+1} \sum_{s=1}^n 4(1-y_s^2)p_n(y_s)U_{k-1}(y_s) \\ &= \begin{cases} 2b_k - b_{k-2} - b_{k+2}, & 2 \leq k \leq n-1, \\ 3b_k - b_{k+2}, & k = 1, \\ 3b_k - b_{k-2}, & k = n. \end{cases} \end{aligned} \quad (\text{B.5})$$

On the other hand, it follows from a direct computation based on orthogonality that

$$\frac{4}{\pi} \int_{-1}^1 p_n(x)U_{k-1}(x)\sqrt{1-x^2}dx = 2\delta_{n,k} + i\delta_{k,n-1}. \quad (\text{B.6})$$

Coupling the above two equations yields a sparse pentadiagonal linear system

$$S_n \mathbf{b} := \begin{pmatrix} 3 & 0 & -1 & & \\ 0 & 2 & 0 & -1 & \\ -1 & 0 & 2 & 0 & -1 \\ & \ddots & \ddots & \ddots & \ddots \\ & & -1 & 0 & 2 & 0 & -1 \\ & & & -1 & 0 & 2 & 0 \\ & & & & -1 & 0 & 3 \end{pmatrix} \begin{pmatrix} b_1 \\ b_2 \\ b_3 \\ \vdots \\ b_{n-2} \\ b_{n-1} \\ b_n \end{pmatrix} = \begin{pmatrix} 0 \\ 0 \\ 0 \\ \vdots \\ 0 \\ i \\ 2 \end{pmatrix}. \quad (\text{B.7})$$

Let $\Psi = [\psi_{jk}]$. The whole fast inversion algorithm for computing $W = \Phi^{-1}$ is given as the following three steps.

Step-1: solve $\mathbf{b} = [b_1, \dots, b_n]^\top$ from (B.7), which costs $\mathcal{O}(n)$ operations by the fast Thomas algorithm.

Step-2: Based on the fact $\psi_{j,n+1} = 0$, the j -th row $\psi_j = [\psi_{j,1}, \dots, \psi_{j,n}]$ of Ψ can be solved from a sequence of sparse tridiagonal linear systems (for each $j = 1, 2, \dots, n$)

$$G_j \psi_j^\top := \text{Tridiag}\{1, -2x_j, 1\} \psi_j^\top = \frac{2}{p'_n(x_j)} \mathbf{b}, \quad (\text{B.8})$$

which in total also costs $\mathcal{O}(n^2)$ operations based on the fast Thomas algorithm for each system.

Step-3: $W = \frac{1}{2} \Psi S_n$, which also needs $\mathcal{O}(n^2)$ operations since S_n is a sparse matrix.

In summary, the dense complex matrix $W = \Phi^{-1}$ can be computed with $\mathcal{O}(n^2)$ complexity.

References

1. A. O. H. Axelsson and J. G. Verwer, *Boundary value techniques for initial value problems in ordinary differential equations*, Math. Comp. **45** (1985), 153–171.
2. L. Brugnano, F. Mazzia, and D. Trigiante, *Parallel implementation of BVM methods*, Appl. Numer. Math. **11** (1993), 115–124.
3. L. Brugnano and D. Trigiante, *Solving differential problems by multistep initial and boundary value methods*, Gordon and Breach Science Publ., Amsterdam, 2003.
4. R. Buchholz, H. Engel, E. Kammann, and F. Tröltzsch, *On the optimal control of the Schlögl-model*, Comput. Optim. Appl. **56** (2013), 153–185.
5. Ed Bueler, *PETSc for partial differential equations: Numerical solutions in C and Python*, SIAM, 2020.
6. Gayatri Caklovic, Robert Speck, and Martin Frank, *A parallel implementation of a diagonalization-based parallel-in-time integrator*, arXiv preprint arXiv:2103.12571 (2021).
7. D. Calvetti and L. Reichel, *Fast inversion of Vandermonde-like matrices involving orthogonal polynomials*, BIT Numer. Math. **33** (1993), 473–484.
8. F. Chen, J. S. Hesthaven, and X. Zhu, *On the use of reduced basis methods to accelerate and stabilize the Parareal method*, in: Reduced Order Methods for Modeling and Computational Reduction, vol. 9, Springer, Berlin, 2014, pp. 187–214.
9. D.L. Chopp, *Introduction to high performance scientific computing*, SIAM, 2019.
10. X. Dai and Y. Maday, *Stable parareal in time method for first- and second-order hyperbolic systems*, SIAM J. Sci. Comput. **35** (2013), A52–A78.
11. Federico Danieli, Ben S Southworth, and Andrew J Wathen, *Space-time block preconditioning for incompressible flow*, arXiv preprint arXiv:2101.07003 (2021).
12. P. Deufhard, *Newton methods for nonlinear problems: affine invariance and adaptive algorithms*, Springer, Berlin, 2004.
13. M. Emmett and M. L. Minion, *Toward an efficient parallel in time method for partial differential equations*, Comm. App. Math. Comp. Sci. **7** (2012), 105–132.
14. R. D. Falgout, S. Friedhoff, T. V. Kolev, S. P. MacLachlan, and J. B. Schroder, *Parallel time integration with multigrid*, SIAM J. Sci. Comput. **36** (2014), C635–C661.
15. C. Farhat, J. Cortial, C. Dastillung, and H. Bavestrello, *Time-parallel implicit integrators for the near-real-time prediction of linear structural dynamic responses*, Int. J. Numer. Methods Eng. **67** (2006), 697–724.
16. L. Fox, *A note on the numerical integration of first order differential equations*, Quart. J. Mech. Appl. Math. **3** (1954), 367–378.
17. L. Fox and A. R. Mitchell, *Boundary value techniques for the numerical solution of initial value problems in ordinary differential equations*, Quart. J. Mech. Appl. Math. **10** (1957), 232–243.
18. M. J. Gander and L. Halpern, *Time parallelization for nonlinear problems based on diagonalization*, Lect. Notes Comput. Sci. Eng. **116** (2017), 163–170.
19. M. J. Gander, L. Halpern, J. Rannou, and J. Ryan, *A direct time parallel solver by diagonalization for the wave equation*, SIAM J. Sci. Comput. **41** (2019), A220–A245.
20. A. Goddard and A. Wathen, *A note on parallel preconditioning for all-at-once evolutionary PDEs*, Electron. Trans. Numer. Anal. **51** (2019), 135–150.
21. I. Gohberg and V. Olshevsky, *Fast inversion of Chebyshev–Vandermonde matrices*, Numer. Math. **67** (1994), 71–92.
22. ———, *The fast generalized Parker–Traub algorithm for inversion of Vandermonde and related matrices*, Journal of Complexity **13** (1997), 208–234.
23. ———, *Fast inversion of Vandermonde and Vandermonde-like matrices*, Communications, Computation, Control, and Signal Processing, Springer, 1997, pp. 205–221.
24. S. Güttel and J. W. Pearson, *A spectral-in-time Newton–Krylov method for nonlinear PDE-constrained optimization*, doi:10.1093/imanum/drab011.

25. N. J Higham, *Fast solution of Vandermonde-like systems involving orthogonal polynomials*, IMA J. Numer. Anal. **8** (1988), 473–486.
26. Nicholas J Higham, *Accuracy and stability of numerical algorithms*, SIAM, 2002.
27. X. Lin, M. Ng, and H. Sun, *A separable preconditioner for time-space fractional Caputo-Riesz diffusion equations*, Numer. Math. Theor. Meth. Appl. **11** (2018), 827–853.
28. J. L. Lions, Y. Maday, and G. Turinici, *A “parareal” in time discretization of PDE’s*, C. R. Acad. Sci. Paris Sér. I Math. **332** (2001), 661–668.
29. J. Liu and S. L. Wu, *A fast block α -circulant preconditioner for all-at-once systems from wave equations*, SIAM J. Matrix Anal. Appl. **41** (2020), 1912–1943.
30. Y. Maday and E. M. Rønquist, *Parallelization in time through tensor-product space-time solvers*, C. R. Acad. Sci. Paris Sér. I Math. **346** (2008), 113–118.
31. E. McDonald, J. Pestana, and A. Wathen, *Preconditioning and iterative solution of all-at-once systems for evolutionary partial differential equations*, SIAM J. Sci. Comput. **40** (2018), A1012–A1033.
32. M. Neumüller and I. Smears, *Time-parallel iterative solvers for parabolic evolution equations*, SIAM J. Sci. Comput. **41** (2019), C28–C51.
33. H. Nguyen and R. Tsai, *A stable parareal-like method for the second order wave equation*, J. Comput. Phys. **405** (2020), 109156.
34. J. M. Ortega and W. C. Rheinboldt, *Iterative solution of nonlinear equations in several variables*, SIAM, Philadelphia, PA, USA, 2000.
35. L. Reichel and G. Opfer, *Chebyshev-vandermonde systems*, Math. Comput. **57** (1991), 703–721.
36. D. Ruprecht, *Wave propagation characteristics of Parareal*, Comput. Visual Sci. **59** (2018), 1–17.
37. D. Ruprecht and R. Krause, *Explicit parallel-in-time integration of a linear acoustic-advection system*, Comput. Fluids **59** (2012), 72–83.
38. J. Steiner, D. Ruprecht, R. Speck, and R. Krause, *Convergence of parareal for the Navier-Stokes equations depending on the reynolds number*, Lect. Notes Comput. Sci. Eng. **103** (2015), 195–202.
39. S. L. Wu, *Convergence analysis of the Parareal-Euler algorithm for systems of ODEs with complex eigenvalues*, J. Sci. Comput. **67** (2016), 644–668.